

Interconnect Failure due to Cyclic Loading

Robert R. Keller[†], Reiner Mönig, Cynthia A. Volkert, Eduard Arzt, Ruth Schwaiger, and Oliver Kraft

Max-Planck-Institut für Metallforschung, Seestr. 92, D-70174 Stuttgart, Germany

[†]National Institute of Standards and Technology, Materials Reliability Division, 325 Broadway, Boulder, CO 80305 U.S.A.

Abstract. The damage generated by AC currents at 100 Hz in interconnects has been studied and compared with mechanical fatigue damage in thin films. The nature of the damage under the two loading conditions is qualitatively similar, supporting the idea that the AC current damage comes from mechanical cycling due to temperature swings on the order of 100 K from Joule heating in the interconnects. In both cases, the damage forms as surface wrinkles within single grains grow in amplitude and extent with time. The possible threat to the reliability of microelectronic and micro-electromechanical systems is further escalated by the observation that soft encapsulation layers do nothing to retard the formation of the damage.

INTRODUCTION

Metallizations in microelectronic devices and micro-electromechanical systems (MEMS) are subjected to a wide variety of time-varying mechanical loading modes, which can potentially induce failures that are not easily predicted through knowledge of monotonic thin film behavior. For instance, power cycling of microelectronic devices due to user operation or energy conservation schemes can lead to significant repetitive thermal strains. In MEMS structures, loading can occur during the repeated action or bending associated with hinged pieces, gears, or cams. In these low frequency applications, mechanical reliability can be compromised because of the consequences of cyclic deformation near surfaces and interfaces. In microelectronic devices, interconnect cross-sections can change, internal stresses can increase, or metal/dielectric delamination can result. In MEMS, cracking or excessive friction may develop.

Direct extrapolation of cyclic mechanical behavior from monotonic testing is generally not feasible, since the damage evolution processes in the two cases are very different. Plastic strain localization becomes more significant in the cyclic case. Complicating matters is the fact that cyclic deformation in small-scale structures is not a well-documented phenomenon. For the case of wide (25 μ m) unencapsulated aluminum lines, Philofsky *et al.* [1] showed 30 years ago that AC current testing can

lead to surface damage associated with slip band formation. The strains in this case are due to temperature cycling, which can easily reach an amplitude of greater than several tens of degrees Kelvin at low frequencies [2]. For the case of blanket metal films, thermal cycling has often been used in conjunction with wafer curvature measurements to study stress evolution, see *e.g.* [3]. Such testing is, however, incapable of separating temperature and stress effects, and is not amenable to large numbers of cycles. Thin film tensile testing has been used with more success to evaluate fatigue behavior in thin films, *e.g.* [4]. Hommel *et al.* [5] showed recently how thin film tensile testing could be used to study cyclic mechanical behavior through the use of compliant polymer substrates.

We consider in this work two types of low frequency cyclic deformation in thin films and interconnects: alternating current (AC)-induced thermal straining of patterned Al interconnects and repeated mechanical loading of Cu and Al films on compliant polymer substrates. The cyclic deformation induced by these forms of loading will be shown to be very similar, despite their origins being considerably different. The focus of this paper is to illustrate surface damage, effects of adjacent materials, and lifetime behavior in cyclically deformed lines and films. Further experimental details are included in [5,6].

ALTERNATING CURRENT-INDUCED DEFORMATION

Several studies in the literature have illustrated that AC currents can lead to severe damage in interconnects [1,6]. The effect is believed to be thermal mechanical fatigue that originates from the cyclic thermal strains due to Joule heating in the interconnects. In this section, the time evolution of damage due to AC currents in Al interconnects, as well as the influence of line width, current density, and various encapsulating layers, is presented.

AC tests were carried out on single level structures that were composed of single Al-1 at. %Si lines, 800 μm long, 0.55 μm thick, and 1.3, 3.3, or 13 μm wide. The lines connected two bond pads and were deposited directly onto oxidized silicon. Tests were carried out on unencapsulated lines, those coated with 2.0 μm of hard-baked photoresist, and those coated with 0.3 μm of reactively sputtered silicon nitride. Each die was attached to a chip carrier using silver paint and the bond pads were connected by ultrasonic wire bonding.

Electrical stressing was performed in a vacuum of approximately 6×10^{-4} Pa (4.5×10^{-6} torr). A signal generator was used to supply the lines with sinusoidal currents at 100 Hz, with DC offsets of less than several mV. Current densities reported in this work refer to the rms current, and are thus a factor $1/\sqrt{2}$ of the maximum current. The sample temperature was monitored using a thermocouple as well as using rms and time-resolved 4 point resistance measurements of the interconnects. The thermocouple, which was attached to the ceramic chip carrier, showed a temperature increase of roughly 100 K during electrical testing of 3.3 μm wide lines at 10 MA/cm^2 .

The carrier temperature is a lower bound for the cycling line temperature. Resistance values provided a more localized measurement of line temperatures. During each half cycle, the time-resolved resistance values indicated a temperature amplitude of approximately 100 K (also measured at 10 MA/cm² on 3.3 μm lines at 100 Hz), with cycling occurring between approximately 120 and 220°C. Resistance was also used to monitor damage formation during testing; it increased due to heating at the beginning of each test and then remained constant until it rapidly increased just before failure occurred by open circuit.

Fig. 1 shows surface damage in an unpassivated 3.3 μm wide Al-1at.%Si line, after 9×10^6 AC current cycles (corresponding to 1.8×10^7 temperature cycles during 25 hours of testing at 100 Hz) at 11 MA/cm², or after, at which point it failed by open circuit. At a given time during the course of any test, one observes regions that are not at all damaged as well as regions with damage ranging from very slight to very severe. The surface damage shown in Fig. 1(a) is typical of some of the less-severely-damaged regions. Periodic surface wrinkles are observed with a spacing of the order of 0.5 μm. Fig. 1(b) shows an example of more severe damage, where the surface wrinkles are larger in amplitude and extend over a larger area. In this case, the wrinkle spacing is approximately 0.25 μm and large extrusions have formed at the sides of the line. Fig. 1(c) shows the site where the open circuit occurred. The characteristic wrinkles are present on either side of the break in the line and there is evidence (such

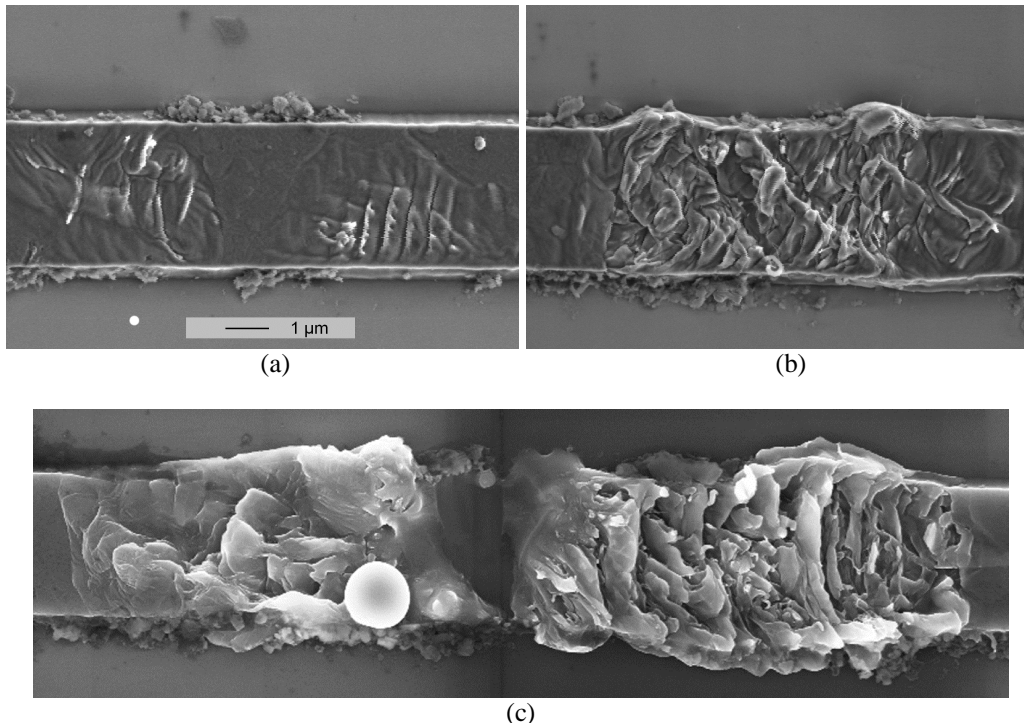


FIGURE 1. 3.3 μm wide unpassivated Al-1at.%Si line after 9×10^6 AC cycles at 100 Hz and an rms current density of 11 MA/cm². Region (a) is only lightly damaged, while region (b) is more severely damaged. Region (c) shows the site where open failure of the line occurred. All images are shown at the same magnification.

as the circular droplet to the left of the break) indicating that the line locally melted just before failure.

Fig. 2 shows FIB images of a 3.3 μm wide Al-1at.%Si line that was tested at 10 MA/cm^2 for approximately 6.5×10^6 AC cycles (18 hours at 100 Hz). The channeling contrast in the images shows the grains in the line, which have a diameter of roughly 2 μm . Similar grain sizes were observed by FIB in the contact pads and in untested lines. For lightly damaged regions such as the one shown here, the damage appears to be contained within a single grain. Fig. 2(b) shows a cross-sectional cut through the line. The underlying SiO_2 layer and Si wafer are clearly visible, as well as the fact that the Al is very thin ($< 0.1 \mu\text{m}$) in the troughs of the wrinkles. There are no voids present at the interface between the metal and the underlying substrate. This is in contrast to what is observed in the mechanically cycled films, as will be seen later in the paper.

In order to investigate the effect of encapsulating layers on the formation of surface damage, AC tests were also run on lines encapsulated with hard-baked photoresist or with a silicon nitride film at 100 Hz and an rms current of 11 MA/cm^2 . The line encapsulated with 2 μm of photoresist was tested for 4.6×10^5 AC current cycles. After the test, the photoresist was dissolved using acetone and the Al surface observed by scanning electron microscopy. The surface morphology on the photoresist-encapsulated sample was indistinguishable from that seen on unpassivated lines, indicating that the photoresist layer did nothing to hinder the formation of damage. The sample encapsulated with 0.3 μm of silicon nitride was tested for 1.3×10^5 AC current cycles. The nitride did not adhere well to the Al as can be seen from the cross-sectional FIB images in Fig. 3. The surface wrinkles caused the nitride layer to both bow away and separate from the metal. In addition, FIB cross-sections suggest that the nitride may have reacted with the Al in several local regions along the line. Further studies are underway to elucidate the effect of hard encapsulants, by growing well-adhering overlayers.

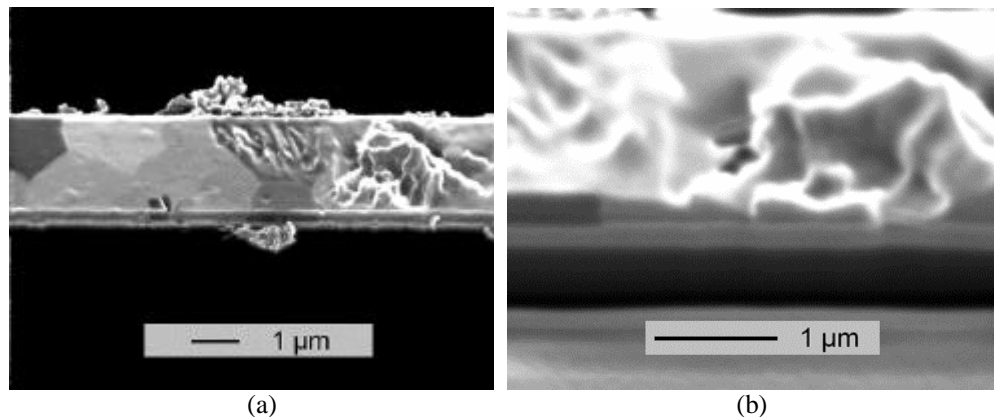


FIGURE 2. FIB images of a 3.3 μm wide Al-1at.%Si line after 6.5×10^6 AC cycles at 100 Hz and an rms current density of 10 MA/cm^2 , (a) at a tilt angle of 30° and (b) at a tilt angle of 45° after cross-sectioning along the line.

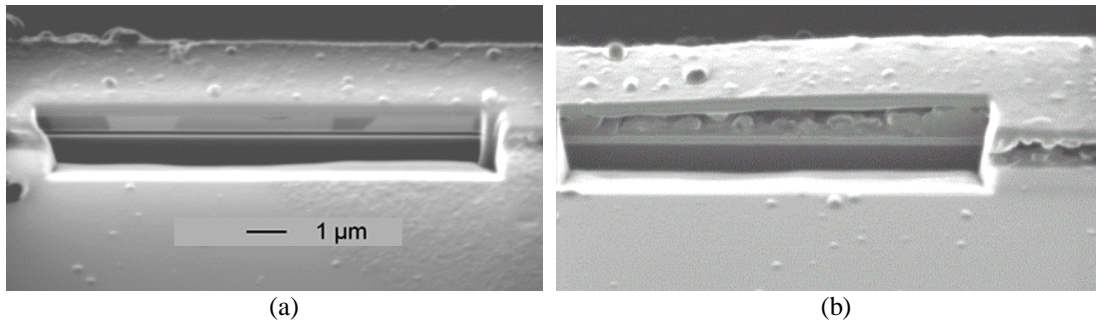


FIGURE 3. Silicon nitride-encapsulated, 3.3 μm wide Al-1at.%Si line (a) before and (b) after 1.3×10^5 AC cycles at 100 Hz and an rms current density of 11 MA/cm^2 . Sample sectioned and imaged by focussed ion beam microscopy. Note bowing and fracture of overlayer as well as damage on surface of line. Images are shown at same magnification.

In some of the lines, sub-micron wide whiskers were found after testing. They were observed only at sites where surface wrinkles were also present. Fig. 4 shows a typical example: several whiskers, including a long, curved one of approximate diameter 50 nm, have grown from a site where surface wrinkles have formed. In general, it seems that whiskers formed somewhat more often in the wider lines and those in wider lines tended to grow much longer than those in narrower lines. Whether this is due to differences in microstructure or mechanical properties or to the fact that the wider lines were tested at lower current densities is not yet clear.

It is difficult to quantify the overall extent of damage as a function of testing time, linewidth, and current density, because of the varying severity of damage found within a single line. However, some rough trends can be observed. With increasing time under stress, the total surface area that is damaged increases, the amplitude of the wrinkles increases, and the spacing of the wrinkles decreases. Eventually, the damage is severe enough that it leads to an electrical open, presumably by local heating resulting from local thinning.

Some similar trends can be established in regard to the effect of current density. Increasing current density leads to increasing surface area of damaged metal and increasing amplitude of the wrinkles. Whether wrinkle spacing decreases remains uncertain. Increasing current density also leads to shorter times to open circuit. At lower current densities, a smaller fraction of the surface area of a line exhibits damage; this behavior persists until open circuit. However, those regions that do undergo changes can become severely damaged. Such areas sometimes show whisker formation.

The effect of linewidth on damage morphology is less clear although some trends can be observed despite the small number of tests performed in this preliminary work. In both wide and narrow lines, damage first begins in isolated regions of the line. These regions are roughly the size of single grains and, as expected for purely geometrical reasons, span a greater fraction of the linewidth in narrower lines. The transition from a damaged region to an undamaged region is less distinct for the case of narrower lines. Finally, the wrinkles are generally more regularly spaced and their amplitude seems considerably larger in the wider lines. In most cases, lines were tested until they failed by open circuit. In general, the higher the current density, the sooner

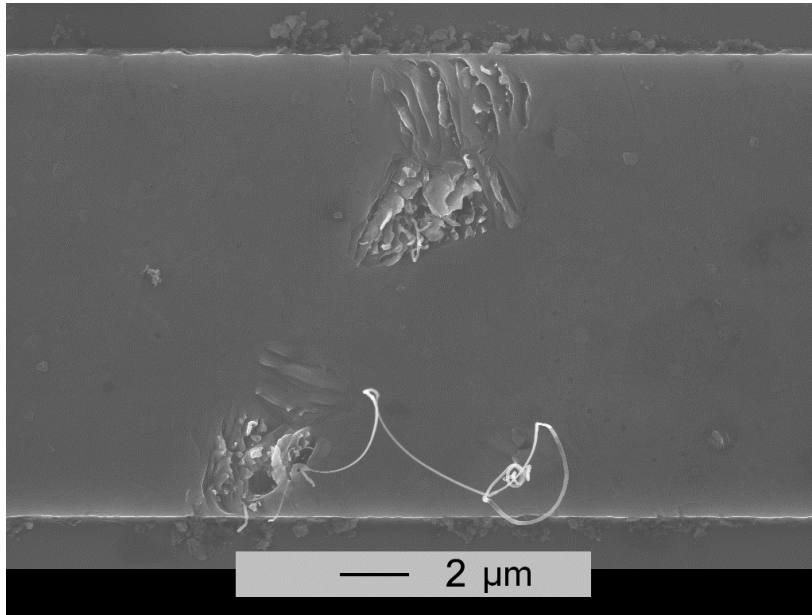


FIGURE 4. Whisker formation in 13 μm wide Al-1at.%Si line after 7.5×10^7 AC cycles at 100 Hz and an rms current density of 5.9 MA/cm^2 .

the lines failed. Given the small number of tests performed on the effect of linewidth, obvious trends were not clear, but it may be that the narrower lines required a larger current density to reach failure within a given number of cycles than the wider lines. Particularly in comparing tests performed using different current densities or linewidths, the time to reach an electrical open is not necessarily a direct measure of the time required to reach a certain level of damage severity. In defining failure for the purposes of measuring lifetime, it may be more useful to quantify the extent of damage in terms of a fraction of the surface area that has become damaged. Whether this leads to lifetime determinations that reveal clearer trends with current density or linewidth than those seen using time to open circuit remains to be seen.

CYCLIC MECHANICAL-INDUCED DEFORMATION

In the following, the damage morphology that results from cyclic mechanical deformation of continuous films is described. For these tests, Al and Cu films were sputter-deposited onto compliant polymer substrates, and the samples subjected to cyclic tensile loading. During these cycles, the substrate material is deformed elastically while the film undergoes plastic deformation in both tension and compression. The method and details of the sample preparation have been described elsewhere [5]. Owing to the sample structure, the film stress cannot be determined from the externally applied load. Therefore, the stress-strain behavior of the films is analyzed using *in-situ* X-ray diffraction during straining of the samples [5,7]. Figure 5

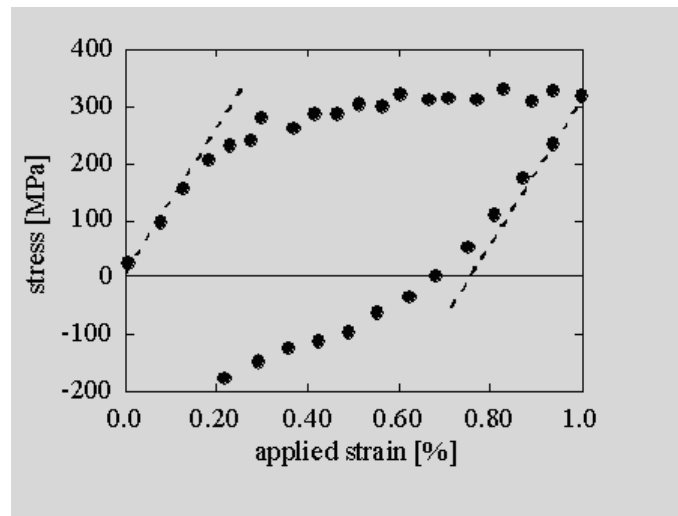


FIGURE 5. Stress-strain behavior of a 1 μm thick Cu film on a 125 μm thick polyimide substrate during a single cycle at room temperature. The film stress was measured by X-ray diffraction.

shows the first cycle from such a tensile test on a 1 μm thick Cu film. On loading, the stress increases linearly with applied strain. The film deforms elastically, as indicated by the dashed line, up to a strain of about 0.15 % and stress of almost 200 MPa. On further loading, the stress-strain behavior is no longer linear and the film is plastically deformed. Due to strain hardening the film stress increases to more than 300 MPa. On unloading of the sample, the substrate contracts and the applied strain is reduced, driving the film into compression. As a result, the film stress first decreases elastically (dashed line) and then makes a transition from elastic to plastic behavior. It has been shown by Kraft *et al.* [8] that this technique can be used for fatigue testing of thin metal films by repeating this cyclic test many times. After testing, damaged regions consisting of cracks and wrinkles were distributed over the entire film. For example, Fig. 6 shows a region of fatigue damage in a 1.0 μm thick Cu film, which was prepared under the same conditions as the one from Fig. 5, but cycled 10,000 times at a frequency of 0.1 Hz rather than just once. One can clearly see the periodic wrinkles formed within single grains, as well as an intergranular crack running from the top to the bottom of the images. The wrinkles have an amplitude of several 100 nm. Careful studies of the wrinkled grains using cross-sectional FIB imaging show that the grains are slightly extruded out of the film and that voids had formed at the interface to the substrate. As the number of cycles increased, the area fraction of damaged regions in the film increased and eventually saturated before the entire surface was damaged. Macroscopic failure or fracture of the samples did not occur, presumably due to the underlying elastic substrate.

In order to compare the damage morphology of the Al interconnects stressed by an AC current to the mechanical fatigue damage in Al films, a 0.5 μm thick Al film on a polyimide substrate was tested. This sample was fatigued with a total strain range of about 0.8% at a frequency of 10 Hz up to 10^6 cycles. The damage in the Al film was very similar to that in the Cu film. Figure 7 (a) shows a FIB micrograph of a damaged

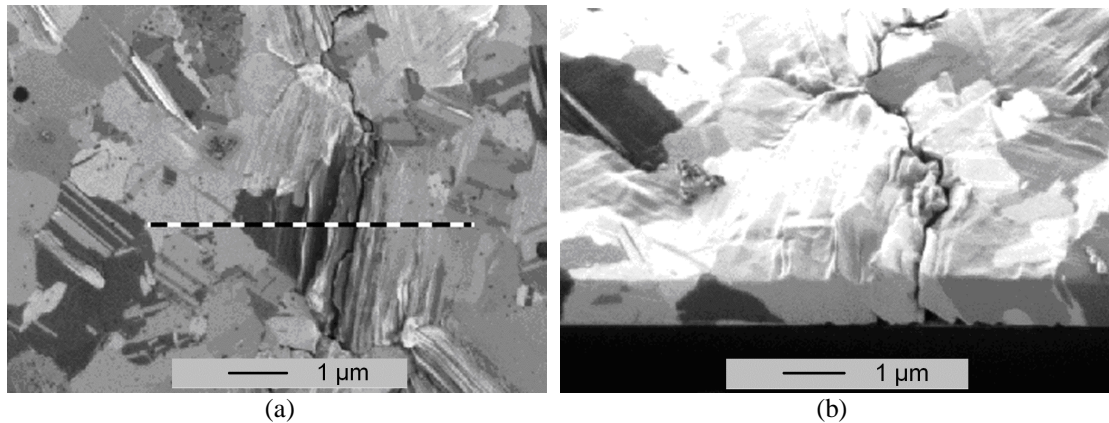


FIGURE 6. FIB micrographs showing the fatigue damage in 1 μm thick Cu films after 10^4 cycles at 0.1 Hz with a total strain range of 1.0%: (a) plan-view image and (b) cross-section at an angle of 45° . The cross-section was prepared at the position marked in (a) by the dashed line. The loading direction was horizontal with respect to the micrographs.

region in the Al film. Surface wrinkles and intergranular cracks can be seen. A cross-section of such a damaged region (Fig. 7 (b)) reveals that the wrinkles are confined to a single grain and that large voids have formed at the interface to the substrate, as for the case of Cu. The height of the wrinkles is similar to the ones found in Cu, but the distance between the individual wrinkles is somewhat larger in the Al than in the Cu. This might be related to the presence of the native oxide on the Al surface.

For both the Al and Cu films, the observations are consistent with the following damage evolution during cyclic mechanical deformation: First, extrusions and voids are formed in individual grains, and then, intergranular cracks originate from these voids. This picture is supported by the fact that many damaged single grains were found which contained wrinkles and voids but were not connected to cracks. As the

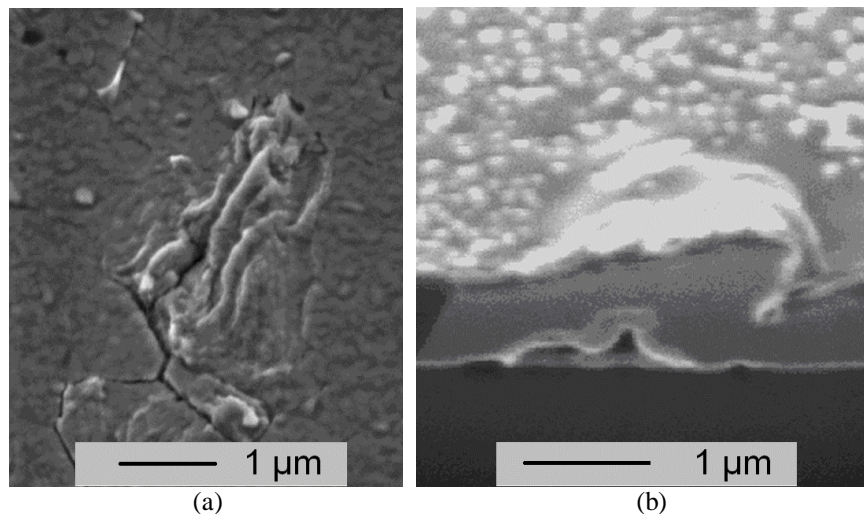


FIGURE 7. FIB micrographs showing the fatigue damage in a 0.5 μm thick Al film after 10^6 cycles at 10 Hz with a total strain range of 0.8%: (a) plan-view image and (b) cross-section at an angle of 45° . The loading direction in the fatigue test was horizontal with respect to the micrographs.

number of cycles increases, the number of damaged grains and cracks also increases. Macroscopic failure of the films did not occur because of the supporting, elastic substrate.

CYCLIC DEFORMATION IN FILMS AND INTERCONNECTS

The damage that results from AC current testing of interconnects and from cyclic mechanical testing of films has been presented in the preceding sections and many similarities are apparent. This is not too surprising since, as stated above, the observed damage created by AC currents has been attributed to thermal mechanical cycling from Joule heating in the interconnects. Possible contributions from electromigration are believed to be small [1,6]. Although it is well known that sufficiently large DC currents lead to electromigration damage, the damage generated by AC currents is viewed as negligible in comparison [9]. This is generally attributed to the idea that the early stages of electromigration damage are reversible and no net damage accumulation occurs under pure, symmetrical AC testing conditions [10]. In addition, at the frequencies used here, the time during a single cycle is too short for significant atomic diffusion to occur. Therefore, the severity of the observed damage is expected to be controlled by the amplitude of the thermal stresses generated by the alternating current. Heating within a line undergoing AC cycling scales with the input power and thus with the square of the current. The actual temperature of the line depends on the efficiency of heat dissipation, which is determined by line geometry and the surrounding materials. The resistance measurements revealed that the 3.3 μm lines cycle between roughly 120 and 220°C at an rms current density of 10 MA/cm². A 100 K temperature increase represents a 210 MPa decrease in film stress, assuming biaxial, anisotropic elastic behavior in (111)-textured Al. X-ray diffraction measurements of the residual biaxial stress in a blanket film portion of the samples resulted in a room temperature value of 270 MPa. Therefore, assuming elastic behavior, the stress would cycle between approximately +60 and -150 MPa during testing of the 3.3 μm lines at 10 MA/cm². Variations in linewidth will change the temperature of the samples, with narrower lines exhibiting both lower average temperatures and smaller temperature amplitudes since they dissipate less power at a given current density. Thus, the exact stresses experienced during current cycling will depend on the linewidth. In addition, variations in current density will change the stress amplitude, with higher current densities driving the stress more compressive and increasing the stress amplitude.

The results from the AC testing can be summarized and compared with literature data for bulk samples using a stress-lifetime (Wöhler, or S-N) plot in Fig. 8. For these samples, the stress amplitude shown was calculated from the cyclic temperature amplitude for each current density as calibrated by resistance measurements. The failure condition was defined as an open circuit. The smooth curve represents data for

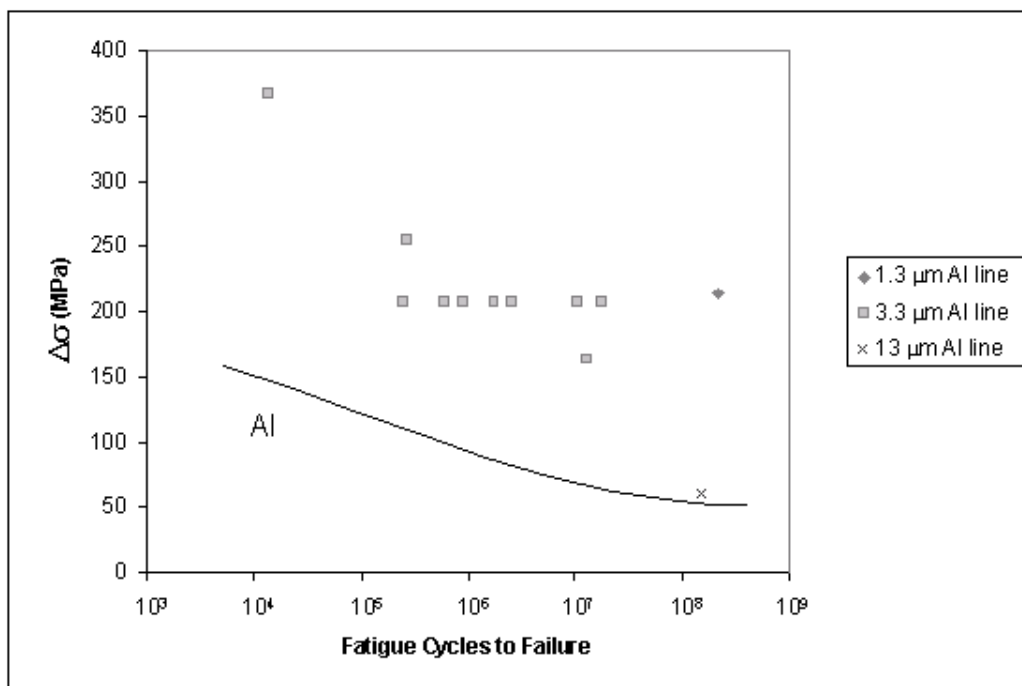


FIGURE 8. Stress amplitude vs. lifetime for AC tested unpassivated Al-1at.%Si lines cycled at 100 Hz. The smooth curve represents fatigue behavior of bulk, fine-grained Al (curve reprinted from reference 11: Acta Metallurgica, vol. 19, A.W. Thompson and W.A. Backofen, "The Effect of Grain Size on Fatigue," pp. 597-606, Copyright (1971), with permission from Elsevier Science).

fatigue of bulk fine-grained Al (20 μm) [11], where failure occurred by macroscopic cracking of the samples. At a given number of cycles, the bulk samples fail at roughly half the stress amplitude required to fail the line samples. However, the general dependence of the number of cycles to failure on stress amplitude is similar for lines and bulk aluminum. There is no evidence of a distinct threshold in stress for inducing fatigue damage in any of the samples. This is consistent with the idea that fatigue can occur even for stresses that are quite a bit lower than the macroscopic yield strength, since significant localized plasticity can occur both in polycrystalline films [12] and in bulk metals (high-cycle fatigue).

Although lifetime data was not collected for fatigued films, it became apparent that the films could also sustain considerably higher stress amplitudes than bulk metals. Several factors may account for the differences in stress amplitude among lines, films, and bulk samples. First, the bulk data was collected for aluminum with a grain diameter of 20 μm , whereas the Al films and lines had an approximate grain diameter of 0.5 μm . While fatigue crack initiation in Al is not strongly grain-size-dependent [11], there is a slight improvement in fatigue life with decreasing grain size. Second, Al films exhibit enhanced yield strengths due to constrained dislocation activity in thin films [12,13]. They can therefore sustain larger stresses at a given applied strain and will experience less plastic strain during cycling. Third, failure defined by cycles to open circuit is not the same as failure defined by cycles to macroscopic cracking. No

fatigue cracks were observed in the lines; localized melting was observed instead. Melting presumably occurred when the cross section of the line decreased to some critical value either because of crack formation or because of local plasticity. Cracks were observed in the thin film on polyimide samples but due to the support of the underlying substrate, did not result in immediate failure. In addition, the substrate could act to suppress the strain localization processes that are known to contribute to fatigue fracture by limiting the total amount of displacement in each cycle. In the absence of a Si or polyimide substrate, perhaps more macroscopic displacements could have been developed, thereby making crack formation easier. Fourth, the stress amplitudes in the interconnects were determined assuming biaxial elastic behavior. While this is likely appropriate for the 13 μm lines, it is less applicable to the 3.3 and 1.3 μm lines [14]. Use of uniaxial elastic constants would lower the stress amplitudes considerably and predict a more tensile average stress. Finally, there is some uncertainty in the temperature measurements during AC testing, which translates to uncertainty in stress. Modifications are in progress to improve the accuracy of the temperature measurement.

There are many similarities to be found between the damage evolution of Al lines/films and bulk Al. In early stages of testing of the films and lines, damage takes the form of subtle surface wrinkles that are widely spaced and show little vertical displacement (amplitude). Such damage takes place only in certain grains, and is reminiscent of what is seen in early stages of fatigue of bulk metals, where dislocation intersections with the free surface leave slip traces. Detailed crystallographic analysis would confirm whether the selectivity in initial damage sites correlates to grains of favorable orientation for slip. With further straining, more damage in the lines and films is seen, in the form of a larger surface area fraction covered in wrinkles, greater amplitude, and narrower spacing. This also occurs in bulk metals, where more grains begin to yield, due to either strain hardening or to slip transmission across boundaries between a yielded and an unyielded grain. Greater surface wrinkle amplitude occurs as strains are accumulated when dislocations intersect and leave a grain. An increasing dislocation density leads to narrower slip band spacing, due to operation of additional dislocation sources and the onset of multiple slip system activity.

There are several differences in the damage observed in the AC tested lines and the mechanically tested thin films. For example, after fatigue testing of the thin films, voids were found in the interface between the metal and the substrate, for both Cu and Al. This is in contrast to what is observed in room temperature fatigue cracking of bulk metals, and also in AC-tested lines, neither of which shows evidence of void formation. Schwaiger and Kraft [16] have suggested that void nucleation in thin films may occur by dislocation annihilation processes during cyclic straining, and that such processes play an important role in thin film fatigue. Dislocation annihilation as a mechanism for increasing the concentration of non-equilibrium point defects such as vacancies has been discussed as a possible contributor to damage by Essmann *et al.* [17] for the case of fatigue in bulk Cu. The fact that voids are seen only in the fatigue-tested metal thin film samples may be a consequence of the metal/polyimide interface itself, which may act as a preferred nucleation site for voids. Another reason such

voids are not observed in AC-tested lines could be that the lines are strained under considerably higher temperatures, often in excess of 200°C, where the overall mobility of point defects is increased. At elevated temperatures, the point defects may have time to move to grain boundaries or to other interfaces and thus avoid reaching a critical supersaturation for void nucleation.

A second difference between the damage observed in the lines and the thin films is the presence of whiskers: whiskers were observed protruding from the AC tested lines but not from the thin films. It is possible, in contrast to void formation, that elevated temperatures favor whisker growth, which would explain their absence in the room temperature tested thin films. The exact mechanism for the whisker growth is not known, but is likely driven by the presence of compressive stresses during cycling. The fact that whiskers were found more often in wide lines than narrow ones might be because the stresses are more compressive in the wider lines. Larger compressive stresses could result from a more biaxial stress state or from larger temperatures and temperature amplitudes.

As discussed above, the presence of both soft and hard overlayers did nothing to retard the formation of fatigue damage during AC testing. Fatigue crack initiation is highly dependent upon surface roughness, including that which develops during cyclic deformation. It has been shown that crack initiation can be suppressed by coating a metal with a hard overlayer [18,19]. The effect in this case is that topography induced by dislocations reaching the free surface is greatly reduced, as long as the overlayer remains intact. As a result, stress concentrations that lead to crack formation do not develop nearly so quickly. However, the experiment presented here, with a silicon nitride overlayer, did not show the expected suppression of surface damage, probably because the layer was not well adherent. Similarly, the relatively soft photoresist overlayer also did nothing to suppress damage formation. The photoresist did remain adherent during testing, but the surface roughness formation was likely unconstrained by the soft polymer. Since hard-baked photoresist is mechanically similar to some materials now under consideration as low-k dielectrics, AC-induced cyclic deformation may well become a problem in such interconnect systems. In addition, power dissipation will always be present in the interconnects of devices, and so will temperature cycles. When low-k interlevel dielectrics (with corresponding low thermal conductivities) and more metallization layers are introduced into devices, the temperature swings will increase and fatigue may become a very serious reliability threat.

SUMMARY

Observations of damage due to AC currents in Al interconnects have been presented and are attributed to thermal mechanical fatigue from the cyclic temperatures generated by Joule heating. The AC current-induced damage is compared with mechanical fatigue damage in Cu and Al thin films on polyimide substrates, and in most respects looks very similar. In both kinds of samples, the damage is similar to that observed at the surfaces of fatigued bulk specimens. It is therefore concluded that

both thin films and interconnects are susceptible to classical fatigue damage, which is generated by the back and forth glide of dislocations. Given the proximity of the surfaces and interfaces in the interconnect and thin film samples, dislocation motion and annihilation is expected to be different from that in bulk material. In particular, sample dimensions may play an important role in determining the nature of the damage that is formed.

The temperature swings generated by the AC currents are typical of those in devices under operating conditions. Based on the fatigue behavior of bulk samples, it is expected that an adherent hard overlayer would inhibit surface fatigue damage formation and a soft overlayer would do little to inhibit damage formation. This may explain the fact that fatigue damage in interconnects encapsulated with well-adhering hard layers such as silicon dioxide or silicon nitride has not been commonly observed. However, if the interconnects are encapsulated with a soft material such as a polymer film, fatigue damage formation may no longer be hindered and failure due to fatigue may occur under normal device operating conditions.

ACKNOWLEDGEMENTS

We thank the NIST Office of Microelectronic Programs and the Max-Planck Visiting Scientist Program for support and Dr. D. Balzar for assistance with X-ray measurements.

REFERENCES

1. Philofsky, E., Ravi, K., Hall, K., and Black, J., "Surface Reconstruction of Aluminum Metallization – a New Potential Wearout Mechanism," in *9th Annual Proceedings of Reliability Physics*, IEEE, New York, 1971, pp. 120-128.
2. Gui, X., Haslett, J.W., Dew, S.K., and Brett, M.J., *IEEE Trans. Electron Dev.* **45**, 380-386 (1998).
3. Sinha, A.K. and Sheng, T.T., *Thin Solid Films* **48**, 117-126 (1978).
4. Read, D.T., *Int. J. Fatigue* **20**, 203-209 (1998).
5. Hommel, M., Kraft, O., and Arzt, E., *J. Mater. Res.* **14**, 2373-2376 (1999).
6. Volkert, C.A., Keller, R.R., Mönig, R., Arzt, E., and Kraft, O., "Fatigue as a Failure Mechanism in Interconnects," to be published (2001).
7. Kretschmann, A., Kuschke, W.-M., Baker, S.P., and Arzt, E., "Plastic Deformation of Thin Copper Films Determined by X-Ray Microtensile Tests," in *Thin Films: Stresses and Mechanical Properties VII*, Mat. Res. Soc. Symp. Proc. Vol. 436, Pittsburgh, 1996, pp. 59-64.
8. Kraft, O., Schwaiger, R., and Wellner, P., to be published in *Mater. Sci. Eng. A*.
9. Rodbell, K.P., Castellano, A.J., and Kaufman, R.I., "AC Electromigration (10 MHz – 1 GHz) in Al Metallization," in *Stress Induced Phenomena in Metallization: Fourth International Workshop*, edited by H.Okabayashi, S.Shingubara, and P.S.Ho, AIP, New York, 1998, pp. 212-223.
10. Shono, K., Kuroki, T., Sekiya, H., and Yamada, H., "Mechanism of AC Electromigration," *Proc. 1990 VMIC Conference*, 1990, pp. 99-105.
11. Thompson, A.W. and Backofen, W.A., *Acta Metall.* **19**, 597-606 (1971).
12. Vinci, R.P., Cornella, G., and Bravman, J.C., "Anelastic Contributions to the Behavior of Freestanding Al Thin Films," in *Stress Induced Phenomena in Metallization: Fifth International Workshop*, edited by O.Kraft, E.Arzt, C.A.Volkert, P.S.Ho and H.Okabayashi, AIP, New York, 1999, pp. 240-248.

13. Nix, W.D., *Metall. Trans.* **20A**, 2217-2245 (1989).
14. Dehm, G., Weiss, D., and Arzt, E., *Mater. Sci. Eng. A.* **309-310**, 468-472 (2001).
15. Sauter, A., *IEEE Trans. Components Hybrids & Manufacturing Technology* **15**, 594-600 (1992).
16. Schwaiger, R. and Kraft, O., *Scripta Mater.* **41**, 823-829 (1999).
17. Essmann, U., Gösele, U., and Mughrabi, H., *Phil. Mag.* **A44**, 405-426 (1981).
18. Alden, T.H. and Backofen, W.A., *Acta Metall.* **9**, 352-366 (1961).
19. Stoudt, M.R., Cammarata, R.C., and Ricker, R.E., *Scripta Mater.* **43**, 491 (2000).